THE JOURNAL OF PHYSICAL CHEMISTRY Letters

Letter

pubs.acs.org/JPCL

Expeditious Stochastic Calculation of Random-Phase Approximation Energies for Thousands of Electrons in Three Dimensions

Daniel Neuhauser,[†] Eran Rabani,[‡] and Roi Baer*[,§]

[†]Department of Chemistry and Biochemistry, University of California, Los Angeles California 90095, United States

[‡]School of Chemistry, The Sackler Faculty of Exact Sciences, Tel Aviv University, Tel Aviv 69978, Israel

[§]Fritz Haber Center for Molecular Dynamics, Institute of Chemistry, Hebrew University, Jerusalem 91904 Israel

ABSTRACT: A fast method is developed for calculating the random phase approximation (RPA) correlation energy for density functional theory. The correlation energy is given by a trace over a projected RPA response matrix, and the trace is taken by a stochastic approach using random perturbation vectors. For a fixed statistical error in the total energy per electron, the method scales, at most, quadratically with the system size; however, in practice, due to self-averaging, it requires less statistical sampling as the system grows, and the performance is close to linear scaling. We demonstrate the method by calculating the RPA correlation energy for cadmium selenide and silicon nanocrystals with over 1500 electrons. We find that the RPA correlation energies per electron are largely independent of the nanocrystal size. In addition, we show that a correlated sampling technique enables calculation of the energy difference between two slightly distorted configurations with scaling and a statistical error similar to that of the total energy per electron.

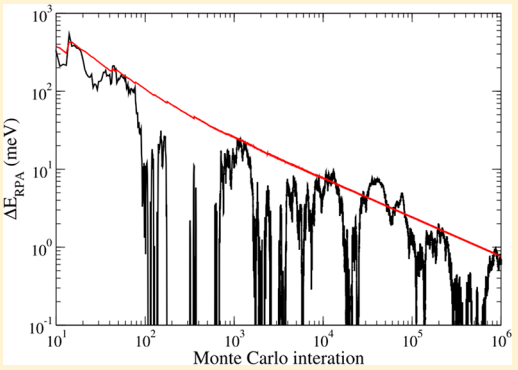

KEYWORDS: *random phase approximation, stochastic iterations, correlation energy, density functional theory*

SECTION: Molecular Structure, Quantum Chemistry, and General Theory

Local and semilocal correlation functionals of Kohn−Sham (KS) density functional theory (DFT) fail to describe long-range van der Waals interactions and other types of dynamical screening effects.[1,2] One route for overcoming these deficiencies is random phase appriximation (RPA) theory[1,3−6] based on the KS-DFT adiabatic connection formalism[7−9] in combination with the fluctuation dissipation theorem.[10] In recent years, this approach, especially when combined with exact exchange, was used successfully for treating various ailments of KS-DFT in molecular and condensed matter systems.[5,6,11−18]

The greatest hurdle facing widespread use of RPA is its exceedingly high computational cost. Several approaches have been developed[5,6,13,19,20] for reducing the naïve $O(\tilde{N}^6)$ RPA scaling to $O(\tilde{N}^4)$, ($\tilde{N}$ is a measure of system size); however, this is still expensive. The problem is aggravated when plane-waves or real-space grids are used, suffering from the huge number of unoccupied states and the strong reliance of the RPA energy on the unoccupied energies.[21−23]

In the present Letter, we develop a stochastic sampling method for estimating the RPA correlation energy. Related sampling techniques have been recently developed by us for estimating the rate of multiexciton generation in nanocrystals (NCs),[24] for a linear scaling calculation of the exchange energy,[25] and for overcoming the computational bottleneck in Møller−Plesset second-order perturbation theory (MP2).[26]

RPA, applied on top of a grid or plane-waves calculation, starts from the KS or generalized KS Hamiltonian $\hat{H}_0$, which can be applied to any wave function in linear scaling numerical effort.[27] For a closed-shell system of $2N$ electrons on a grid/basis of size M, the N lowest KS orbitals $\phi_i(r)$ of $\hat{H}_0$ are occupied and $M-N$ are unoccupied.[28] The RPA correlation energy can be written as[5] $E_C^{RPA} = (1/2)\Sigma_{ia,\tilde{\Omega}_{ia}>0}(\tilde{\Omega}_{ia} - A_{ia,ia})$, where $\tilde{\Omega}_{ia}$ are eigenvalues of "$\tilde{L}$" defined by

$$\tilde{L}\begin{pmatrix} X \\ Y \end{pmatrix}_{ak} = \begin{pmatrix} 0 & B-A \\ A+B & 0 \end{pmatrix}\begin{pmatrix} X \\ Y \end{pmatrix}_{ak} = i\tilde{\Omega}_{ak}\begin{pmatrix} X \\ Y \end{pmatrix}_{ak} \quad (1)$$

and

$$A_{ka,jb} = 2W_{ka,jb} + \delta_{kj}\delta_{ab}\omega_{kj}$$
$$B_{ka,jb} = 2W_{ka,jb} \quad (2)$$

where $W_{pq,st} = \lambda\int(\phi_p(r)\phi_s(r')\phi_t(r')\phi_q(r)/|r - r'|)d^3r\ d^3r'$ are the Coulomb integrals, λ is a coupling strength parameter ($\lambda = 1$ is full-strength Coulomb coupling and $\lambda = 0$ is the noninteracting limit), and $\omega_{st} = \varepsilon_s - \varepsilon_t$ is the difference of eigenvalues of $\hat{H}_0$. Note that the eigenvalues $\tilde{\Omega}_{ak}$ are real, even though $\tilde{L}$, although having pure imaginary eigenvalues, is a real

Received: December 26, 2012
Accepted: March 8, 2013
Published: March 8, 2013

matrix operating on real vectors $\begin{pmatrix} X \\ Y \end{pmatrix}$. Note that $\tilde{\Omega}_{ia}$ are also the eigenvalues of the matrix $\begin{pmatrix} A & B \\ -B & -A \end{pmatrix}$ appearing in standard RPA treatments.[5]

An alternative formulation starts from the expression[5]

$$E_C^{RPA} = \frac{1}{2}\left[\tilde{R}(1) - \left(\tilde{R}(\lambda) + \frac{d\tilde{R}}{d\lambda}\right)_{\lambda=0}\right] \tag{3}$$

where $\tilde{R}(\lambda) \approx (1/2)\Sigma_{ia,}\tilde{\Omega}_{ia>0}(\lambda)$. However, the calculation of $\tilde{R}(\lambda)$ is still prohibitive for large systems because of the high cost of diagonalization of the $2N(M-N) \times 2N(M-N)$ $\tilde{L}$ matrix (in grid representations, M and N easily reach 10^6 and 10^4, respectively).

Our formulation is based on a linear-response time-dependent Hartree approach.[29,30] E_C^{RPA} is still given by eq 3, but $\tilde{R}(\lambda)$ is replaced by the following trace:[29,30]

$$R(\lambda) \equiv tr[\Omega^+(\hat{L}(\lambda))] \tag{4}$$

Here $\Omega^+(x) = x\theta(x)$, where $\theta(x)$ is the Heaviside step function, which we approximate as $\theta(x) \approx (1/2)\mathrm{erfc}(-\beta x)$; $\hat{L}$ is a *linear operator*, revealed when linearizing the time-dependent KS equations (see refs 14 and 30 for details):

$$\hat{L}\begin{pmatrix} \chi_k \\ \Upsilon_k \end{pmatrix} = \begin{pmatrix} -(\hat{H}_0 - \varepsilon_k)\Upsilon_k \\ v_H[\Delta\rho]\phi_k + (\hat{H}_0 - \varepsilon_k)\chi_k \end{pmatrix} \tag{5}$$

$\chi_k(r)$ and $\Upsilon_k(r)$ are functions, originally describing the time-dependent Hartree response of the kth KS orbital $\phi_k(r)$, but are used here as stochastic perturbations as detailed below. $v_H[\Delta\rho](r) = \lambda\int(\Delta\rho(r')/|r - r'|)d^3r'$ is the Hartree perturbation potential depending linearly on the χ's via

$$\Delta\rho(r) = 4\sum_{j=1}^{N}\phi_j(r)\chi_j(r) \tag{6}$$

One can expand $\hat{L}$ in the basis of the KS orbitals and obtain its $2NM \times 2NM$ matrix $L_{pq,st}$ having NM positive imaginary eigenvalues $i\Omega_{st}$ and an equivalent negative set. $N(M-N)$ eigenvalues can be classified as "occupied−unoccupied" transitions Ω_{ka}, and N^2 eigenvalues are occupied−occupied transitions Ω_{kj}. Obviously, the dimensions of L and $\tilde{L}$ differ, as the latter describes only occupied−unoccupied transitions. Nonetheless, within the occupied−unoccupied space, the matrices and eigenvalues are identical:[31]

$$L_{ka,jb} = \tilde{L}_{ka,jb},\ \Omega_{ka} = \tilde{\Omega}_{ka} \tag{7}$$

$R(\lambda)$ in eq 4 is computed in three principal steps:

(1) The trace is replaced by an average (denoted by curly brackets) over random perturbation vectors $\begin{pmatrix} \chi \\ \Upsilon \end{pmatrix}$:

$$R(\lambda) = \left\{(\chi \quad \Upsilon)\left|\Omega^+(\hat{L}(\lambda))\right|\begin{pmatrix} \chi \\ \Upsilon \end{pmatrix}\right\} \tag{8}$$

$\begin{pmatrix} \chi \\ \Upsilon \end{pmatrix}$ is shorthand notation for the entire set of χ_k's and Υ_k's.

(2) The selection of the random vector χ_k and Υ_k is done by generating two vectors composed of random complex phases at each grid point r_g: $\zeta_{1,2}(r_g) = (1/h^{3/2})e^{i\theta_{1,2}(r_g)}$, where h is the grid spacing and $\theta_{1,2}(r_g)$ is a random number between 0 and 2π. Then one sets:

$$\chi_k(r_g) + i\Upsilon_k(r_g) = \zeta_1(r_g)\langle\zeta_2|\psi_k\rangle - \zeta_2(r_g)\langle\zeta_1|\psi_k\rangle \tag{9}$$

(3) The action of the operator $\Omega^+(i\hat{L})$ on $\begin{pmatrix} \chi \\ \Upsilon \end{pmatrix}$ is performed using an iterative modified Chebyshev polynomial expansion approach, so that

$$R(\lambda) = \sum_{m=0}^{n_c} c_m r_m \tag{10}$$

where

$$r_m = \left\{(\chi \quad \Upsilon)\left|\begin{pmatrix} \chi^{(m)} \\ \Upsilon^{(m)} \end{pmatrix}\right.\right\} \tag{11}$$

are the modified Chebyshev residues, and $\begin{pmatrix} \chi^{(m)} \\ \Upsilon^{(m)} \end{pmatrix}$ are calculated iteratively:

$$\begin{pmatrix} \chi^{(m+1)} \\ \Upsilon^{(m+1)} \end{pmatrix} = \frac{2}{\Delta}\hat{L}\begin{pmatrix} \chi^{(m)} \\ \Upsilon^{(m)} \end{pmatrix} + \begin{pmatrix} \chi^{(m-1)} \\ \Upsilon^{(m-1)} \end{pmatrix} \quad (m > 1) \tag{12}$$

with

$$\begin{pmatrix} \chi^{(0)} \\ \Upsilon^{(0)} \end{pmatrix} = \begin{pmatrix} \chi \\ \Upsilon \end{pmatrix},\ \begin{pmatrix} \chi^{(1)} \\ \Upsilon^{(1)} \end{pmatrix} = \frac{1}{\Delta}\hat{L}\begin{pmatrix} \chi^{(0)} \\ \Upsilon^{(0)} \end{pmatrix} \tag{13}$$

Note that $\hat{L}$ is a real operator (eq 5), so all calculations are done on real functions. $\Delta = (1/2)(l_{max} - l_{min})$ is half the eigenvalue range of $i\hat{L}$. The c_m are numerical coefficients obtained as follows: First, prepare a series of length $4n_c$, $d_n = \Omega^+(\Delta\cos((\pi/2n_c)n))$, $n = 0, ..., 4n_c - 1$, and then set $c_m = (\tilde{d}_m/(4n_c(1 + \delta_{m0})))$ (for $m = 0, ..., n_c$), where $\{\tilde{d}\}$ are the discrete Fourier transform of $\{d\}$. The series length n_c is chosen large enough so that the sum in eq 10 converges, i.e., $|c_{nc}|$ is smaller than a prescribed tolerance.

We rely on correlated sampling to reduce the statistical error in computing E_C^{RPA}. R is computed for three values of $\lambda = 1, +\eta$, and $-\eta$ (with $\eta = 10^{-3}$) using the same random number seeds, and then the RPA energy is estimated by

$$E_C^{RPA} = \frac{1}{2}\left[R(1) - \frac{1}{2}\sum_{\lambda=\pm\eta}\left(1 + \frac{1}{\lambda}\right)R(\lambda)\right] \tag{14}$$

We now demonstrate the performance of the stochastic method by applying it to calculate the RPA correlation energies of spherical cadmium-selenide (CdSe) and hydrogen passivated silicon NCs, where the Hamiltonian $\hat{H}_0$ is constructed from a semiempirical pseudopotential model.[32,33] The N occupied states of the NCs were obtained using the filter diagonalization technique[34] with the implementation described in refs 32 and 35. We used $\beta = 30E_h^{-1}$ for approximating the step function $\Omega^+(x)$, $n_c = 1024$ (see discussion of Figure 4), and $\Delta \approx 12E_h$, slightly larger than half the maximal eigenvalue range for both NCs. Various features of the NCs are summarized in Tables 1 and 2.

dx.doi.org/10.1021/jz3021606 | J. Phys. Chem. Lett. 2013, 4, 1172−1176

Table 1. Parameters for the CdSe NCs[a]

N_{Cd}	N_{Se}	N_e	D (nm)	N_L	E_g (eV)
20	19	152	1.4	2 490 368	3.8
83	81	648	2.1	35 831 808	2.9
151	147	1176	2.5	154 140 672	2.7

[a]Shown are the number of Cd (N_{Cd}) and Se (N_{Se}) atoms, electrons (N_e), NC diameter (D), the numerical effort involved in operating with L on a perturbation vector $N_L = (1/2)N_e \times N_g$, where N_g is the number of grid-points and E_g is the occupied−unoccupied energy gap.

Table 2. Same as Table 1, but for Hydrogen Passivated Silicon NCs

N_{Si}	N_H	N_e	D (nm)	N_L	E_g (eV)
1	4	8		6912	10.7
35	36	176	1.3	2 883 584	3.9
87	76	424	1.6	23 445 504	3.2
353	196	1608	2.4	210 763 776	2.2

As a test, we compared the stochastic estimate and a full summation calculation of the RPA energy for SiH_4 on a 8 × 8 × 8 point grid (see Figure 1). The deviation of the stochastic approach from the exact value is within the statistical variance for nearly all stochastic iterations. We found that for 10 000 stochastic iterations, the stochastic estimate deviates by ∼10 meV from the full summation value. As explained below, the number of required stochastic iterations decreases considerably (for a fixed error per electron) as the size of the system increases.

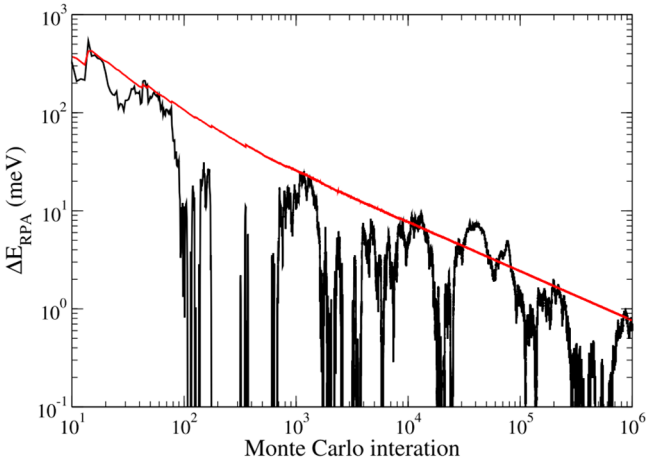

Figure 1. The error of the stochastic estimate for the RPA energy per electron with respect to the exact value (black curve) and the variance (red curve) as function of stochastic iterations for SiH_4.

Figure 2 shows the RPA correlation energies for CdSe and silicon NCs up to ≈1600 electrons along with a comparison to MP2 energies obtained using the Neuhauser−Rabani−Baer (NRB) method.[26] The RPA correlation energy is much less sensitive to the NC size when compared to MP2. This is because the NC gaps decrease with system size, and MP2 energies are sensitive to small gaps (diverging for metals). The RPA energy of silicon is somewhat above that of CdSe, and is within the LDA bulk limit[21] range of 1 − 1.5 eV.

The insets of Figure 2 show the corresponding statistical errors normalized to 1000 stochastic iterations. The errors decrease when the number of electrons in the system increases.

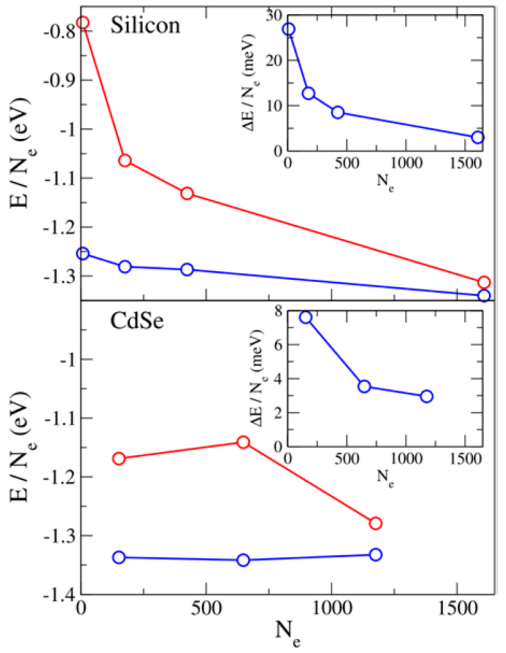

Figure 2. RPA (blue) and MP2 (red) correlation energies per electron vs the number of electrons N_e, for silicon (top) and CdSe (bottom) NCs. Insets show the statistical errors in the RPA energies, normalized to 1000 stochastic iterations.

This shows that the algorithm profits from statistical self-averaging. The statistical error of the CdSe NCs is approximately twice smaller than that for silicon despite having similar gaps for the same NC size. This suggests that the statistical errors are not trivially correlated with the gap.

Figure 3 shows the total CPU time for calculations that yield a statistical error of ≈10 meV per electron. The method scales,

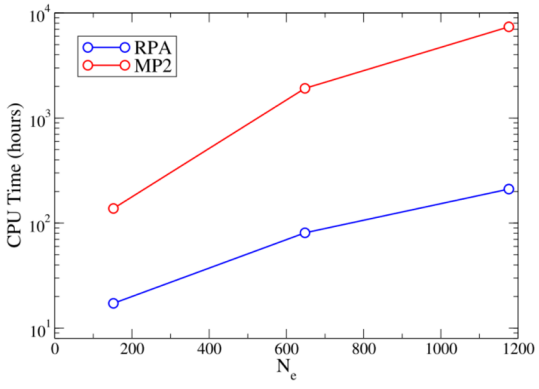

Figure 3. The CPU times for achieving a statistical error of ≈10 meV per electron for the RPA and MP2 calculations of CdSe NCs.

at most, quadratically with system size but in practice, due to self-averaging, requires considerably less statistical sampling as the system grows, and the resulting performance is close to *linear scaling*. Furthermore, in comparison, the RPA CPU time for the same statistical error is an order of magnitude smaller than the CPU time required for the MP2 calculations. Regarding memory requirements, for the RPA scales quadratically with system size (17 GB for the largest silicon NC) and linearly for MP2.

In some cases, the Chebyshev interpolation suffers from instabilities. This is shown in the Figure 4 for the $Si_{353}H_{196}$ NC,

dx.doi.org/10.1021/jz3021606 | J. Phys. Chem. Lett. 2013, 4, 1172−1176

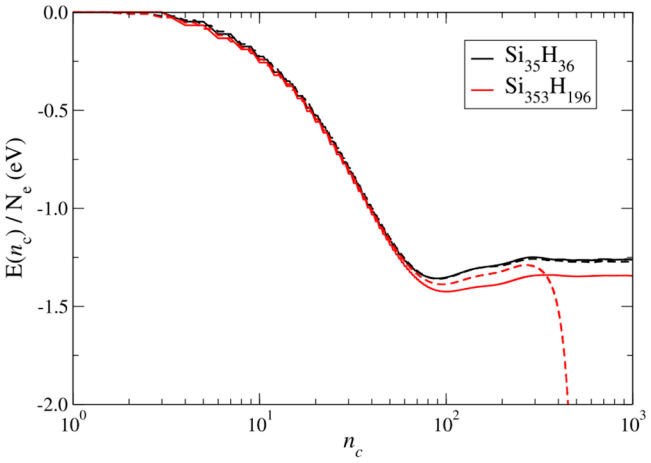

Figure 4. The RPA correlation energy as function of the length of the Chebyshev interpolation polynomial for silicon NCs. Dashed lines are the results without projection, while the solid lines are for $n_p = 0$ for $Si_{35}H_{36}$ and $n_p = 10$ for $Si_{353}H_{196}$.

where we plot the RPA energy estimate as a function of the length of the Chebyshev expansion. The results (dashed line) clearly diverge as the Chebyshev expansion length grows. To alleviate this problem, we follow each operation of $\hat{L}$ on $\binom{X_k^{(m+1)}}{Y_k^{(m+1)}}$ by a projecting out the operands the "close by" occupied orbitals ψ_j, $j = k - n_p$, ..., $k + n_p$ where n_p is a small system-dependent integer.

Figure 4 shows the RPA correlation energy as a function of the Chebyshev interpolation order (n_c). For $Si_{35}H_{36}$ the RPA energy with ($n_p = 0$) and without projection are nearly identical (to within statistical error). For higher interpolation orders than shown, the RPA correlation energy without projection diverges while the projected one remains stable. For $Si_{353}H_{196}$, the Chebyshev polynomial visibly diverges already when the order is larger than 300 but becomes stable when projection is used with $n_p = 10$. Here too, the difference between the projected and nonprojected correlation energies (before divergence) is smaller than the statistical fluctuations, which is large in the diverged result due to the small number of stochastic iterations done.

The present method is not only useful to calculate the RPA energy per electron. In fact, it can also be used to obtain, for example, the RPA corrections to chemical reaction energy profiles or to adsorption energies. In this respect, we have developed an approach, based on a combination of adiabatic evolution and correlated sampling to calculate energy differences between two structural configurations.[36] Preliminary results for SiH_4 (enabling comparison to the full summation result) and $Si_{35}H_{36}$, moving one atom by $0.01a_0$, indicate that the statistical error of the energy gradient (i.e., the force due the RPA energy) is comparable to the statistical error of the total RPA energy per electron (much smaller than the statistical error in the total energy). For SiH_4 and $Si_{35}H_{36}$, the statistical error per stochastic iteration[37] in the RPA energy is 0.016 and 0.05 eV, respectively, compared to the statistical error in the RPA energy per electron 0.25 and 0.15 eV, respectively.

Summarizing, we have presented a new stochastic approach for calculating RPA energies for large electronic systems of exceptional size. The method scales formally as $O(\tilde{N}^2)$ in terms of memory and CPU time but due to self-averaging has a near-linear scaling CPU time performance. We calculated the RPA correlation energy for CdSe and silicon NCs up to diameters of 2.5 nm with over 1500 electrons. The stochastic approach developed here bloats, by orders of magnitude, the size of systems that can be treated using RPA theory.

AUTHOR INFORMATION

Notes

The authors declare no competing financial interest.

ACKNOWLEDGMENTS

D.N. was supported by the DOE MEEM center, award DE-SC0001342. R.B. was supported by the U.S.−Israel Binational Foundation (BSF). R.B. and E.R. gratefully thank the Israel Science Foundation, Grant Numbers 1020/10 and 611/11, respectively.

REFERENCES

(1) Perdew, J. P.; Schmidt, K. In *Density Functional Theory and Its Application to Materials*; Van Doren, V. E., Van Alsenoy, C., Geerlings, P., Eds.; AIP Conference Proceedings, Antwerp, Belgium, 8−10 June 2000;American Institute of Physics: Melville, NY, 2001.
(2) Marom, N.; Tkatchenko, A.; Rossi, M.; Gobre, V. V.; Hod, O.; Scheffler, M.; Kronik, L. *J. Chem. Theor. Comput.* **2011**, *7*, 3944.
(3) Janesko, B. G.; Henderson, T. M.; Scuseria, G. E. *J. Chem. Phys.* **2009**, *131*, 034110.
(4) Fuchs, M.; Gonze, X. *Phys. Rev. B* **2002**, *65*, 235109.
(5) Eshuis, H.; Bates, J. E.; Furche, F. *Theor. Chem. Acc.* **2012**, *131*, 1084.
(6) Ren, X. G.; Rinke, P.; Joas, C.; Scheffler, M. *J. Mater. Sci.* **2012**, *47*, 7447.
(7) Langreth, D. C.; Perdew, J. P. *Solid State Commun.* **1975**, *17*, 1425.
(8) Gunnarsson, O.; Lundqvist, B. I. *Phys. Rev. B* **1976**, *13*, 4274.
(9) Langreth, D. C.; Perdew, J. P. *Phys. Rev. B* **1977**, *15*, 2884.
(10) Callen, H. B.; Welton, T. A. *Phys. Rev.* **1951**, *83*, 34.
(11) Andersson, Y.; Langreth, D. C.; Lundqvist, B. I. *Phys. Rev. Lett.* **1996**, *76*, 102.
(12) Dobson, J. F.; Wang, J. *Phys. Rev. Lett.* **1999**, *82*, 2123.
(13) Paier, J.; Ren, X.; Rinke, P.; Scuseria, G. E.; Gruneis, A.; Kresse, G.; Scheffler, M. *New J. Phys.* **2012**, *14*, 043002.
(14) Baer, R.; Neuhauser, D. *J. Chem. Phys.* **2004**, *121*, 9803.
(15) Scuseria, G. E.; Henderson, T. M.; Sorensen, D. C. *J. Chem. Phys.* **2008**, *129*, 231101.
(16) Angyan, J. G.; Liu, R. F.; Toulouse, J.; Jansen, G. *J. Chem. Theor. Comput.* **2011**, *7*, 3116.
(17) Paier, J.; Janesko, B. G.; Henderson, T. M.; Scuseria, G. E.; Gruneis, A.; Kresse, G. *J. Chem. Phys.* **2010**, *132*, 094103.
(18) Schimka, L.; Harl, J.; Stroppa, A.; Gruneis, A.; Marsman, M.; Mittendorfer, F.; Kresse, G. *Nat. Mater.* **2010**, *9*, 741.
(19) Rocca, D.; Bai, Z.; Li, R.-C.; Galli, G. *J. Chem. Phys.* **2012**, *136*, 034111.
(20) Ren, X. G.; Rinke, P.; Scheffler, M. *Phys. Rev. B* **2009**, *80*, 045402.
(21) Nguyen, H. V.; de Gironcoli, S. *Phys. Rev. B* **2009**, *79*, 205114.
(22) Harl, J.; Kresse, G. *Phys. Rev. B* **2008**, *77*, 045136.
(23) Lu, D.; Nguyen, H.-V.; Galli, G. *J. Chem. Phys.* **2010**, *133*, 154110.
(24) Baer, R.; Rabani, E. *Nano Lett.* **2012**, *12*, 2123.
(25) Baer, R.; Neuhauser, D. *J. Chem. Phys.* **2012**, *137*, 051103.
(26) Neuhauser, D.; Rabani, E.; Baer, R. *J. Chem. Theor. Comput.* **2012**, *9*, 24.
(27) The numerical effort of the stochastic RPA calculation scales quadratically with system size provided the numerical effort involved in applying the underlying Hamiltonian to a wave function scales linearly with system size. This happens when the underlying Hamiltonian is derived from KS DFT since the potential is local. Furthermore, it will also be true for a generalized KS DFT Hamiltonian having short-range

exchange. When long-range exchange is present in the Hamiltonian, it is considerably more difficult to apply the Hamiltonian to a wave function in a linear scaling way.
(28) We denote occupied states by indices i, j, k, l = 1, ..., N and unoccupied states by a, b, c, d = N + 1, ..., M; the indices p, q, s, t = 1, ..., M denote "unrestricted" states.
(29) Neuhauser, D.; Baer, R. *J. Chem. Phys.* **2005**, *123*, 204105.
(30) Baroni, S.; de Gironcoli, S.; Dal Corso, A.; Giannozzi, P. *Rev. Mod. Phys.* **2001**, *73*, 515.
(31) The occupied−occupied eigenvalues, although affecting R will not affect the RPA correlation energy calculated by eq. 3. A proof will be given in a future publication.
(32) Rabani, E.; Hetenyi, B.; Berne, B. J.; Brus, L. E. *J. Chem. Phys.* **1999**, *110*, 5355.
(33) Wang, L. W.; Zunger, A. *J. Phys. Chem.* **1994**, *98*, 2158.
(34) Wall, M. R.; Neuhauser, D. *J. Chem. Phys.* **1995**, *102*, 8011.
(35) Toledo, S.; Rabani, E. *J. Comput. Phys.* **2002**, *180*, 256.
(36) Details of this approach will be described in a future publication.
(37) To estimate the statistical error for I stochastic iterations divide by the square root of I.